

This is the peer reviewed version of the following article: Cornacchia L, Wharton G, Davies G, Grabowski RC, Temmerman S, van der Wal D, Bouma TJ, van de Koppel J. (2020) Self-organization of river vegetation leads to emergent buffering of river flows and water levels. Proc. R. Soc. B 287: 20201147. <http://dx.doi.org/10.1098/rspb.2020.1147>. This article may be used for non-commercial purposes in accordance with the publisher's Terms and Conditions for Self-Archiving.

Self-organization of river vegetation leads to emergent buffering of river flows and water levels

Authors:

Loreta Cornacchia ^{a, f}	Loreta.Cornacchia@nioz.nl
Geraldene Wharton ^b	G.Wharton@qmul.ac.uk
Grieg Davies ^c	Grieg.Davies@southernwater.co.uk
Robert C. Grabowski ^d	R.C.Grabowski@cranfield.ac.uk
Stijn Temmerman ^e	Stijn.Temmerman@uantwerpen.be
Daphne van der Wal ^{a, g}	Daphne.van.der.Wal@nioz.nl
Tjeerd J. Bouma ^{a, f, h}	Tjeerd.Bouma@nioz.nl
Johan van de Koppel ^{a, f}	Johan.van.de.Koppel@nioz.nl

Affiliations:

a: NIOZ Royal Netherlands Institute for Sea Research, Department of Estuarine and Delta Systems, and Utrecht University, P.O. Box 140, 4400 AC Yerseke, the Netherlands.
b: School of Geography, Queen Mary University of London, London, UK
c: Southern Water Services, Southern House, Worthing, UK
d: Cranfield Water Science Institute, Cranfield University, Cranfield, UK
e: Ecosystem Management Research Group, University of Antwerp, Universiteitsplein 1, 2610 Wilrijk, Belgium
f: Groningen Institute for Evolutionary Life Sciences, University of Groningen, PO Box 11103, 9700 CC Groningen, The Netherlands
g: Faculty of Geo-Information Science and Earth Observation (ITC), University of Twente, P.O. Box 217, 7500AE, Enschede, The Netherlands
h: Faculty of Geosciences, Department of Physical Geography, Utrecht University, Utrecht, The Netherlands

Corresponding author:

Loreta Cornacchia
Royal Netherlands Institute for Sea Research
Korringaweg 7
4401 NT Yerseke
The Netherlands
e.mail: loreta.cornacchia@nioz.nl
Tel.: +31 (0)113 577 457
Fax: +31 (0)113 573 616

45 Keywords: bio-physical feedbacks | spatial self-organization | flow regulation | submerged aquatic
46 macrophytes

Abstract

Global climate change is expected to impact hydrodynamic conditions in stream ecosystems. There is limited understanding of how stream ecosystems interact and possibly adapt to novel hydrodynamic conditions. Combining mathematical modelling with field data, we demonstrate that bio-physical feedback between plant growth and flow redistribution triggers spatial self-organization of in-channel vegetation that buffers for changed hydrological conditions. The interplay of vegetation growth and hydrodynamics results in a spatial separation of the stream into densely vegetated, low-flow zones divided by unvegetated channels of higher flow velocities. This self-organization process decouples both local flow velocities and water levels from the forcing effect of changing stream discharge. Field data from two lowland, baseflow-dominated streams support model predictions and highlight two important stream-level emergent properties: vegetation controls flow conveyance in fast-flowing channels throughout the annual growth cycle, and this buffering of discharge variations maintains water depths and wetted habitat for the stream community. Our results provide important evidence of how plant-driven self-organization allows stream ecosystems to adapt to changing hydrological conditions, maintaining suitable hydrodynamic conditions to support high biodiversity.

Introduction

The importance of vegetation in affecting water and air flow and shaping physical landscapes has been widely recognized [1, 2]. Mountain and hillslope vegetation reduces surface runoff, river discharge and erosion rates, thereby affecting landscape morphology [3, 4]; vegetation steers tidal landscape development [5-7] and dune formation [8]; and in-stream, riparian, and floodplain plants affect the processes and forms of alluvial rivers [9-11]. Water flow velocities in rivers are a function of the balance between energy imposed by slope or discharge and the resistance imposed by the river bed. Within shallow, low-energy rivers, submerged and marginal aquatic vegetation imparts a resistance to water flow [12] that affects water velocities in the channel [13-15]. Conventional models, relating river discharge to flow velocity, assume vegetation to be an independent resistance factor restricting water flow [16] with vegetation cover regarded as a static entity, presuming a uni-directional effect of vegetation on water flow. However, aquatic vegetation cover is also controlled by water flow, among other factors (reviewed in [17]); water velocity influences the presence, density and species composition of aquatic vegetation communities [17, 18]. Whilst field surveys [14, 15] and models [19] have highlighted the impact of seasonal variation in vegetation cover in streams on local water velocities, they often ignore the two-way interaction in the process.

Aquatic vegetation typically grows as monospecific patches within streams [17] with a patterning caused by self-organization processes emerging from the divergence of water around vegetation patches [20]. This interaction results in spatial patterns of patch alignment [21] that are important for species facilitation [22]. Although self-organization is recognized as an important regulating process in several natural systems [23], including the morphological structure of fluvial systems [24], there is insufficient understanding of the implications of self-organization induced by the interaction between plant growth and water flow for the functioning of vegetated rivers and streams. Moreover, we know very little about the ability of stream ecosystems to maintain a healthy, diverse ecosystem in the face of changing discharge. This is a pressing need, as these high-biodiversity ecosystems are expected to face more severe hydrological conditions due to global climate change and human modifications of rivers and their catchments.

We present a combined mathematical and empirical investigation that reveals how feedback mechanisms between in-stream plants and river discharge buffer flow velocities and water levels against high and low flows. A model is developed that describes the interplay of plant growth and hydrodynamics within a spatially heterogeneous vegetated stream. With this model, we explore how self-organization processes that emerge from this interaction create heterogeneity in plant biomass and water flow, and how this in turn affects stream hydrodynamic conditions. We model an “abstract” stream where we adopt a simplified setting of a single channelized flow area in between two vegetated areas, and focus on the lateral adjustment of the effective width of the channel in response to increasing discharge (**Fig. 1A**). Moreover, we assume that the stream is groundwater fed and baseflow dominated, and hence discharge is presumed to change gradually. Plant growth is described in the model using the logistic growth equation, and plant mortality due to hydrodynamic stress is assumed to increase linearly with net water velocity [5]. We assume that the lateral expansion of plants through clonal growth can be described by a random walk, and we therefore apply a diffusion approximation [25]. Water flow is modelled using depth-averaged shallow water equations in non-conservative form. The effects of friction exerted by the bed and vegetation on flow velocity are represented by the Chézy coefficient, following the approach of Baptist et al. [26], slightly modified to account for bending of flexible submerged macrophytes in response to increased water flow [27]. To test the model predictions on flow regulation by in-stream plants, we use field measurements of seasonal variations in plant cover, discharge, water levels and spatial patterns of flow velocities within and around vegetation patches in two baseflow-dominated single-thread chalk streams with seasonal variations in discharge. One stream was dominated by mixed submerged and emergent vegetation, and the other by submerged vegetation (see Materials and methods).

Results

(a) Water discharge regulates vegetation cover. Our model analysis reveals that the feedback between vegetation growth and local flow velocity creates a self-organization process that allows vegetation cover to readjust in response to increasing discharge (see bifurcation analysis in electronic supplementary material S1 and Fig. S1; electronic supplementary material S2 and Fig. S2). At low

discharge, the entire stream becomes homogeneously vegetated (**Fig. 1A**). When discharge increases, the equilibrium changes from a homogeneously covered state to a partly covered state where the flow is separated into two distinct spatial zones. One is characterized by low to zero vegetation biomass and high flow velocities in the middle of the stream, and the other by high biomass and low flow velocities at the edges of the stream. This is caused by a scale-dependent effect of vegetation on hydrodynamics where increased flow resistance locally reduces flow velocities in the vegetated regions, while water flow is diverted and concentrated outside of the vegetation, thereby inhibiting its expansion. With steadily increasing discharge, the area of channelled flow progressively increases and the vegetated portions decrease as plants are uprooted, due to the self-organized adjustment of vegetation cover to incoming discharge, until the system shifts to an unvegetated equilibrium where no vegetation can persist (**Fig. 1A**). The resulting inverse relationship between incoming flow discharge and vegetation cover (**Fig. 1B**) was calibrated to best fit the negative relationship observed in the field for both study sites, showing that vegetation cover decreases (as plants are uprooted) with increasing discharge ($R^2 = 0.77$, $p < 0.0001$, **Fig. 1C**) in response to the seasonal pattern of changing hydrology and vegetation growth and die-back. Moreover, our model predictions are supported by experimental evidence of the flow divergence effect of vegetation patches: thus in the zone adjacent to the vegetation, our model predicts on average a flow acceleration of 52% compared to the incoming flow velocity, a value close to the 42% average acceleration reported in [20].

(b) Vegetation regulates flow velocities. The model predicts that local flow velocities both within the vegetation and in the unvegetated channelled flow area are relatively unaffected by changing discharge (**Fig. 2A**). The slopes of the velocity-discharge relationships in Fig. 2A indicate that flow velocities increase by 0.03 m s^{-1} per unit increase in discharge within the vegetation, and by 0.06 m s^{-1} between the vegetation. This stability in local flow velocities is the consequence of the adjustment of vegetation cover to increases in overall water discharge, with vegetation expanding when discharge and flow velocities in the channelled area decrease, and retreating due to uprooting when discharge and flow velocities increase. Hence vegetation readjustment buffers for increased discharge, thereby maintaining relatively constant water flow velocities (**Fig. 2A**). These predictions are supported by

field data at the two study sites. Flow velocities within and between vegetation patches are buffered against changes in discharge. The presence of vegetation alone explains up to five times as much of the variation in the observed flow velocities compared to discharge (electronic supplementary material S3). In comparison, when averaged over the cross-section, water velocities show a much stronger response to discharge variations, as a larger volume of water is passing through the channel. However, since the area covered by vegetation decreases with increasing discharge, the widened, high-flow section of the stream accommodates the increased discharge and a four-fold increase in discharge produces only a slight (although significant) increase in local velocities (**Fig. 2B & 2C**; further details in electronic supplementary material S4 and Fig. S3).

(c) Vegetation regulates water levels. A second property emerging from the two-way interaction between water flow and vegetation growth is that water levels in the channel with self-organized vegetation are maintained at constant level despite increasing discharge (**Fig. 3A**). By increasing hydraulic roughness, vegetation raises water levels compared to an unvegetated stream for a given discharge. This effect is most pronounced at low discharge, where water levels are significantly higher in vegetated compared to unvegetated streams. As discharge increases, however, vegetation cover decreases, producing strikingly constant water levels, whereas water levels would steadily increase in a homogeneously vegetated channel (**Fig. 3A**). These predictions are confirmed by our field measurements of mean water levels from both study sites (**Fig. 3B**). In the ‘mixed vegetation’ site, water levels were on average 0.28 ± 0.04 m, and only increased by 0.09 m for each unit increase in discharge ($r^2 = 0.54$, $p = 0.0003$; **Fig. 3B**), less than half of what would be expected for an unvegetated stream (based on the model simulations in Fig. 3A). In the River Frome, the site with predominantly submerged plants, water levels were on average 0.39 ± 0.07 m, and did not significantly increase with discharge ($r^2 = 0.06$, $p = 0.44$; **Fig. 3B**), in agreement with model predictions. Thus, for both study sites the largest effect of vegetation in raising water levels, relative to an unvegetated stream, occurs at low discharges.

Discussion

Using a combined mathematical modelling and empirical study, we show that aquatic macrophytes can regulate both flow velocities and water levels in baseflow-dominated streams. Regulation results from a self-organization process caused by the bio-physical feedback between vegetation growth and flow redistribution. Here, increases in water discharge cause a decrease in partial cover of aquatic vegetation relative to the unvegetated channels, creating a larger in-channel area for flow conveyance. This self-organized adaptation of the cover of submerged vegetation buffers the impact of an increase in discharge, resulting in relatively constant local flow velocities and water levels independent of discharge. Our study highlights that flow regulation resulting from biophysical feedback mechanisms and self-organization of aquatic vegetation enables lowland stream ecosystems to adapt to changing hydrological regimes, such as those induced by global change.

The two-way interaction between water flow and plant growth has important implications for the functioning of the stream as an ecosystem and the provision of a wide range of ecosystem services. Specifically, it facilitates the maintenance of biodiversity despite increasing discharge that might otherwise create conditions adverse to plant growth. By buffering variations in local water flow velocities, vegetation maintains both low-flow-velocity and high-flow-velocity habitats within individual reaches. This self-organized heterogeneity facilitates ecosystem resilience to discharge variations and increases stream biodiversity [15, 28] by structuring communities of various aquatic organisms. In-stream plants increase habitat complexity and maintain a wide range of mesohabitats for fish species, by providing high-flow areas for feeding and spawning, adjacent to sheltered low-flow areas for nursery, resting, and refuge from predation. Moreover, by preserving reach-scale water depths, water temperatures are lowered and can hold greater dissolved oxygen levels [29], and the high-flow velocities in the channelled areas between vegetation patches increase the turbulent diffusion of atmospheric oxygen into the water. Thus, the survival of a wide range of aquatic and riparian organisms is facilitated. This is crucially important during low summer discharge, where water levels might otherwise be insufficient to maintain a functioning aquatic community [15, 30]. Finally, the creation of fast flowing areas in between the vegetation ensures flow and sediment conveyance when in-stream macrophyte growth is abundant, maintains river bed permeability by

reducing the ingress of fine sediments into river beds [31], and keeps a clean gravel bed as spawning ground for fish [32].

Our model results further highlight two additional important biological implications of the flow regulation process resulting from self-organization, in terms of the adaptive capacity of fluvial ecosystems facing altered discharges due to global climate change or human engineering. *First*, our model predictions indicate that the self-organized vegetation pattern allows vegetation to persist over a wider range of discharges than if it were homogeneously distributed throughout the river bed. These non-linear dynamics lead to a metastable equilibrium between plant resistance and fluvial disturbance in intermediate energy rivers, where the abiotic-biotic feedbacks and self-adjustment processes are strongest [33, 34]. Moreover, within a certain range of discharge, the system has two stable states, one where vegetation is patterned and a bare state where vegetation cannot survive (see electronic supplementary material S1 and Fig. S1). Hence, removal of vegetation due to human management or natural disturbances under conditions of high discharge might shift the system towards the alternative unvegetated state, from which vegetation recovery is slow or severely hindered unless discharge is significantly reduced. A *second* implication of our results is that self-organized pattern formation strongly increases macrophyte resilience compared to homogeneously vegetated streams, in terms of a faster recovery of vegetation biomass following, for instance, a disturbance imposed by strong discharge variations (see electronic supplementary material S5 and Fig. S4). This enhanced resistance and resilience of stream ecosystems resulting from self-organization processes is highly important in the light of global change. Intensification of rainfall [35] in combination with land use change in river catchments [36, 37] may alter hydrologic partitioning and surface runoff, imposing increasingly stressful and variable discharge conditions on stream ecosystems.

Our results, therefore, lead to important considerations for the management of stream ecosystems. In current maintenance strategies, abundant vegetation growth is typically regarded as problematic because it decreases the capacity of these streams for water conveyance in response to high discharge [17, 38]. However, our study provides evidence for the value of submerged aquatic vegetation in rivers which, through a process of self-organization over time, ensures flow conveyance

and maintains sufficient water levels for the aquatic ecological community at low discharges. Hence, there might be a need to reconsider vegetation as an important component of the adaptive capacity of stream ecosystems and their ability to maintain a diverse range of habitats. The empirical results in this study were collected over a 2-year period in two streams that have baseflow-dominated hydrographs with relatively subtle changes in water discharge. Further research is now needed on river systems with flashier hydrological regimes and different aquatic plant species (morphologies, biomechanical properties, and life-history traits) to test the stability and generality of these biophysical feedback dynamics. Future studies also need to examine changes over longer (inter-annual) and shorter (event-based) timescales and explore how changes in river hydrogeomorphology (channel dimensions, sediment transport) and biogeochemistry (nutrient levels) might impact on the reciprocal relationships between vegetation and flow properties.

Spatial patterning generates important emergent effects (e.g. increased productivity, resistance) that go beyond the simple creation of heterogeneity, compared with a non-patterned state [23]. These emergent effects have been increasingly observed in many self-organized ecosystems, suggesting their generality. The process of water flow diversion within self-organizing ecosystems is not unique to streams. Similar vegetation-induced self-organization processes affect hydrodynamics in salt marsh pioneer vegetation [5, 39], diatom-covered tidal flats [40], and flow-governed peat land ecosystems [23, 41]. This points at the universal emergent properties that result from the interplay of vegetation, water flow and drainage, shaping the adaptive capacity of fluvial and intertidal ecosystems and the services these ecosystems deliver in terms of supporting biodiversity. Another implication of our study is that flow velocities are ultimately determined by the maximum flow stress that plants can tolerate before being uprooted. Since plant traits are under evolutionary constraints, this might suggest that physical processes such as water flow can reflect the control of evolutionary processes in biogeomorphic systems. With the current rates of climate change threatening ecosystems worldwide and potentially increasing the frequency and intensity of rainfall, increased insight into the emergent, regulating properties of spatial self-organization in ecosystems and an understanding of their role in

ecosystem resilience will be essential to help maintain natural ecosystems in a future governed by global change.

Materials and methods

(a) Model description. To study how vegetation affects flow velocity and water levels in streams, we constructed a spatially-explicit mathematical model of the interplay of plant growth and water flow through a heterogeneously vegetated stream. The model consists of a set of partial differential equations, where one equation describes the dynamics in two spatial dimensions of plant density (P), and where water velocity and water level are described using the shallow water equations. By only including the essential aspects of the coupling between hydrodynamics and vegetation, our model allows us to investigate the key process of flow velocity and water level regulation by macrophytes.

The rate of change of plant biomass P [g DW m⁻²] in each grid cell is described by:

$$\frac{\partial P}{\partial t} = rP \left(1 - \frac{P}{k}\right) - m_w P |u| + D \left(\frac{\partial^2 P}{\partial x^2} + \frac{\partial^2 P}{\partial y^2} \right) \quad (1)$$

Here, plant growth is described using the logistic growth equation, where r [day⁻¹] is the intrinsic growth rate of the plants and k [g DW m⁻²] is the plant carrying capacity, that indirectly reflects the mechanisms of nutrient and light competition between the plants (see Franklin *et al.* [17] for a review of the main factors controlling macrophyte growth and survival). Plant mortality caused by hydrodynamic stress is modelled as the product of the mortality constant m_w [m⁻¹] and net water speed [m s⁻¹] due to plant breakage or uprooting at higher velocities [5, 17, 42]. As the net water speed is converted in m day⁻¹, the mortality constant is divided by a conversion factor of 86400 to obtain plant mortality in the units of g DW m⁻² day⁻¹. We assume that the lateral expansion of plants through clonal growth can be described by a random walk, and we therefore apply a diffusion approximation, where D [m² day⁻¹] is the diffusion constant of the plants [25].

Water flow is modeled using depth-averaged shallow water equations in non-conservative form [43].

To determine water depth and speed in both x and y directions we have:

$$\frac{\partial u}{\partial t} = -g \frac{\partial H}{\partial x} - u \frac{\partial u}{\partial x} - v \frac{\partial u}{\partial y} - \frac{g}{C_d^2} u \frac{|u|}{h} + \nabla(D_u \nabla u) \quad (2)$$

$$\frac{\partial v}{\partial t} = -g \frac{\partial H}{\partial y} - u \frac{\partial v}{\partial x} - v \frac{\partial v}{\partial y} - \frac{g}{C_d^2} v \frac{|u|}{h} + \nabla(D_U \nabla v) \quad (3)$$

$$\frac{\partial h}{\partial t} = -\frac{\partial}{\partial x}(uh) - \frac{\partial}{\partial y}(vh) \quad (4)$$

where u [m s^{-1}] is water velocity in the streamwise (x) direction, v [m s^{-1}] is the water velocity in the spanwise (y) direction, H [m] is the elevation of the water surface (expressed as the sum of water depth and the underlying bottom topography), h [m] is water depth and C_d [$\text{m}^{1/2}/\text{s}$] is the Chézy roughness coefficient due to bed and vegetation roughness and the terms $\nabla(D_U \nabla u, \nabla v)$ represent turbulent diffusion (with $\nabla = (\frac{\partial}{\partial x}, \frac{\partial}{\partial y})$ and horizontal eddy viscosity $D_U = 0.02 \text{ m}^2 \text{ s}^{-1}$). The effects of bed and vegetative roughness on flow velocity are represented by determining hydrodynamic roughness characteristics for each cover type separately using the Chézy coefficient, following the approach of Straatsma and Baptist [44] and Verschoren *et al.* [27].

The Chézy coefficient within the unvegetated cells of the simulated grid, which we will refer to as C_b in this paper, is calculated using Manning's roughness coefficient through the following relation:

$$C_b = \frac{1}{n} h^{1/6} \quad (5)$$

where n [$\text{s/m}^{1/3}$] is Manning's roughness coefficient for an unvegetated gravel bed channel and h [m] is water depth.

The Chézy coefficient for each grid cell occupied by submerged vegetation, which we will refer to as C_d , is calculated using the equation of Baptist *et al.* [26] and slightly modified by Verschoren *et al.* [27] to account for reconfiguration of flexible submerged macrophytes. Due to the important feedback effects taking place between macrophyte growth and flow velocity [17], we link the hydrodynamic and plant growth model by relating wetted plant surface area to plant biomass, to express vegetation resistance as:

$$C_d = \sqrt{\frac{1}{C_b^{-2} + (2g)^{-1} D_c A_w}} + \frac{\sqrt{g}}{k_v} \ln \frac{h}{H_v} \quad (6)$$

where C_b [$\text{m}^{1/2}/\text{s}$] is the Chézy coefficient for non-vegetated surfaces (Eq. 5), g is acceleration due to gravity (9.81 m s^{-2}), D_c [-] is a species-specific drag coefficient, A_w [$\text{m}^2 \text{ m}^{-2}$] is the wetted plant surface

area (total wetted surface area of the vegetation per unit horizontal surface area of the river [27, 45]), directly related to plant biomass through the empirical relationship described for *Ranunculus* in Gregg and Rose [46], k_v is the Von Kármán constant (0.41 [-]), and H_v [m] is the deflected vegetation height (further defined below). The equation proposed by Baptist *et al.* [26] has been identified as one of the best fitting model to represent the effects of vegetation on flow resistance, for both artificial and real (submerged and emergent) vegetation [47]. Deflected vegetation height varies as a function of incoming flow velocity, due to the high flexibility of submerged aquatic vegetation and reconfiguration at higher stream velocities [45, 48]. Following the approach of Verschoren *et al.* [27], H_v is calculated within each vegetated grid cell as the product of shoot length L [m] and the sine of the bending angle α [degrees] (**Table 1**), using an empirical relationship between bending angle and incoming current velocity based on flume experiments performed on single shoots of *Ranunculus penicillatus* [49]. In our model, bending angle of a single shoot is used to represent the bending angle of a whole patch, as plants located at the leading edge tend to push the whole canopy towards the stream bed. However, bending of the vegetation in a patch with multiple shoots can be expected to decrease with increasing along-stream distance within the patch, due to flow deceleration effects of the vegetation. **Table 1** provides an overview of the parameter values used, their interpretations, units and sources. We were able to obtain parameter values from the literature for all parameters except for r , m_w and D , which were fine-tuned to provide the best quantitative fit to the observed vegetation cover across the discharge gradient. The diffusion rate of plants D , corresponding to an expansion rate of $8.5 \text{ cm}^2 \text{ day}^{-1}$, falls within the range of values reported in [50] ($2 - 150 \text{ cm}^2 \text{ day}^{-1}$). Although our model is principle-seeking and does not aim to generate precise predictions, the robustness of the model for changes in these parameter values is presented in electronic supplementary material S6. Sensitivity analyses revealed that changes in these parameter values resulted in quantitative but not qualitative changes in model behaviour, i.e. the absolute values of flow velocity changed (quantitative changes), but their relationship with discharge (trend of relatively constant velocities) remained unchanged. For parameter values outside of the range tested here, numerical instabilities would arise and produce curvatures in the unvegetated middle channel, an aspect that was out of the focus of this work and was not investigated further.

(b) Study sites. Two lowland, groundwater-fed chalk stream reaches were chosen for a two-year survey of macrophyte growth and flow velocity patterns (**Table 2** and electronic supplementary material, Fig S5). The first reach, on the Bere Stream (50° 44' 11.50" N, 2° 12' 21.42" W), was located within the River Piddle catchment. The second reach, Frome Vauchurch (50° 46' 29.95" N, 2° 34' 18.32" W), was located within the River Frome catchment. Based on the river classification in Rinaldi *et al.* [51], the study sites are single-thread alluvial channels on intermediate (gravel-sand) substrates with straight-sinuuous planform, characterized by an unconfined, low energy setting and groundwater-dominated hydrographs. The two study reaches were selected to provide a comparison in terms of species richness of aquatic macrophyte cover. The Bere Stream reach was selected for its richness in macrophyte cover, while the Frome Vauchurch reach was dominated by *Ranunculus* stands. The study reaches were straight sections of 30 m long by 7-9 m wide. In the Bere Stream ('mixed vegetation site'), the dominant in-channel aquatic macrophyte was water crowfoot (*Ranunculus penicillatus* subsp. *pseudofluitans*), represented in both floating-leaved and submergent forms, whilst the stream margins were mainly colonized by the emergent macrophyte *Nasturtium officinale* (watercress) in similar proportions (bar plot in Fig. 2B). Other macrophyte species, such as *Apium nodiflorum* and *Callitriche* sp., were also present in the channel in sparser stands. In the Frome Vauchurch ('dominant submerged site'), *Nasturtium* was not found and *Ranunculus* was the dominant in-stream macrophyte, representing more than 80% of the total macrophyte cover (bar plot in Fig. 2C).

(c) Field measurements. The two study reaches were mapped throughout two annual growth cycles (July 2008 – July 2010). Field surveys were conducted monthly from July 2008 to July 2009, and bimonthly until July 2010. During each survey, macrophyte distribution and hydrodynamic conditions were mapped along transects that were located at 1-m distance intervals along the 30-m long study reaches. Along each transect, measurement points were located at 0.5 m intervals to measure water depth, macrophyte presence and species, and water flow velocities (m s^{-1}) (see electronic supplementary material, Fig. S6 for an example of a plotted stream cross-section showing the raw field measurements). Total water depth was measured as the depth between the water surface and the

surface of the gravel bed, using a reinforced meter rule. The velocity in each position was measured down from the water surface at 60% of the total flow depth with an electromagnetic flow meter (Valeport Model 801) for 30 seconds, to have an estimate of the depth-averaged flow velocity in the water column [52]. A single measurement at 60% of the water depth was deemed more suitable for the survey than multiple measurements (for example at 80% and 20% of the water depth), as the majority of points measured were generally <0.5 m in total depth [53]. The average flow velocities for the vegetated and unvegetated sections of the channel were calculated for each survey month, based on the cover type of each measurement point. The relationship between discharge and cross-sectional average velocities were calculated for each survey month as the ratio between the measured discharge ($\text{m}^3 \text{s}^{-1}$) and the cross-sectional area (m^2). For comparison, in the main text we present a subset of the monthly measurements from the ‘dominant submerged’ site that fall within the same range of discharge as the ‘mixed vegetation’ site. The full dataset is provided in electronic supplementary material S4 and Fig. S3.

(d) Statistical analyses. The mean vegetated and unvegetated flow velocities for each survey month were compared using Kruskal-Wallis one-way tests. The correlations between channel discharge and mean total water level, and between discharge and vegetated and unvegetated flow velocities in the ‘mixed vegetation’ site, were tested with a linear regression model. The correlation between channel discharge and vegetated and unvegetated flow velocities in the ‘dominant submerged’ site was tested with piecewise regression.

(e) Numerical implementation. We investigated vegetation development with two-dimensional numerical simulations using the central difference scheme on the finite difference equations. The simulated area consisted of a rectangular grid of 600×250 cells, to simulate a straight channel (50 m long, 15 m wide) with rectangular cross-sectional shape and initial bed slope of 0.0007 m m^{-1} . The grid resolution was higher in the spanwise than in the streamwise direction ($\Delta x = 0.08 \text{ m}$, $\Delta y = 0.06 \text{ m}$), as the model predictions revealed only lateral (spanwise) variations in vegetation cover and not in the streamwise direction. Moreover, the grid resolution and the turbulent eddy viscosity ($D_U = 0.02 \text{ m}^2 \text{s}^{-1}$) were chosen to obtain numerically stable solutions according to the mesh Peclet number and the

Courant-Friedrichs-Lewy condition [54]. The grid resolution had limited effect on the solution of the model. Simulations performed with a higher spatial resolution ($\Delta x = 0.04$ m, $\Delta y = 0.03$ m, a grid of 1200×500 cells) showed less than 1% difference in the predicted vegetation cover, water level and flow velocity estimation. The boundary condition downstream was a constant discharge. No flow was assumed through the lateral boundaries and thus the velocity component in the direction normal to the boundary (i.e. cross-stream (y) direction) was set to zero. Although a no-slip boundary condition would be more appropriate to represent bank roughness at the channel edges, it would have required to properly resolve the boundary layer profile, which was out of the scope of our simplified flow model. As flow redistribution processes and the scale-dependent feedback leading to vegetation adjustments mostly occur in the cross-stream direction, we assumed that lateral expansion of vegetation would be mainly affected in the cross-channel direction, rather than along, the channel. Therefore, although the model can simulate vegetation growth in both the streamwise and cross-stream direction, the starting conditions were homogeneous in the streamwise direction: at the beginning of each simulation, vegetation was set to occupy a fixed amount of the channel bed, in the form of two bands located along the channel margins and each occupying 1/3 of the cross-section (see electronic supplementary material Fig. S7 for a visualization of the spatial model output). The final vegetated state was independent of the initial conditions, as was found in other self-organization models [40, 55]. Simulations where the initial vegetation cover was increased in 10% increments resulted in the same final vegetation cover.

An iterative procedure was used to solve the two equations for flow velocity and vegetation biomass. The model simulation started with setting initial conditions for u , v , and P . The streamwise velocity u was set to a uniform velocity of 0.14 m s^{-1} and the spanwise velocity v was set equal to zero. The biomass P was set to 200 g m^{-2} in the two bands along the channel margins. First, the net water speed was calculated based on the initial conditions for u and v . The net water speed was then used to calculate the bending angle of the vegetation and the deflected vegetation height (H_v). Based on the initial values of plant biomass P at the start of the simulation (t_0), the vegetative Chézy roughness was calculated. The change in the water flow velocity in both u and v directions was then calculated based on the Chézy roughness. Finally, given the flow velocities in u and v , the changes in

plant biomass P were calculated. The use of a small time step minimized the effect of computation order on the results. The time step length was set at $dt = 0.01$ days and the end time of the simulation was set at 500 days. All presented simulations generally reached equilibrium at $t = 100$ days. A simulation was considered to have reached equilibrium when the rate of change of plant biomass over time was zero ($dP/dt = 0$).

A total of 25 simulations were undertaken starting with a discharge value of $0.57 \text{ m}^3 \text{ s}^{-1}$. At the end of each simulation, discharge was progressively increased by $0.04 \text{ m}^3 \text{ s}^{-1}$ and the results of the previous simulation were used as initial condition. For each simulation, we calculated the vegetation cover (% of vegetated cells over the simulated domain), the mean flow velocity in the vegetated cells, the mean flow velocity in the unvegetated cells, and the mean water depth over the simulated domain. These values were related to the discharge value in each simulation to produce the relationships in Figures 1 – 3.

Acknowledgements

This work was supported by the Research Executive Agency, through the 7th Framework Programme of the European Union, Support for Training and Career Development of Researchers (Marie Curie - FP7-PEOPLE-2012-ITN), which funded the Initial Training Network (ITN) HYTECH ‘Hydrodynamic Transport in Ecologically Critical Heterogeneous Interfaces’, N.316546. Data collection in the Frome-Piddle catchment, Dorset, was supported by the Natural Environment Research Council (algorithm studentship awarded to Grieg Davies) and Queen Mary University of London (through a university studentship awarded to Bob Grabowski).

References

1. Dietrich W.E., Perron J.T. 2006 The search for a topographic signature of life. *Nature* **439**(7075), 411-418.
2. Corenblit D., Baas A.C., Bornette G., Darrozes J., Delmotte S., Francis R.A., Gurnell A.M., Julien F., Naiman R.J., Steiger J. 2011 Feedbacks between geomorphology and biota controlling Earth surface processes and landforms: a review of foundation concepts and current understandings. *Earth-Science Reviews* **106**(3), 307-331.
3. Istanbuluoglu E., Bras R.L. 2005 Vegetation-modulated landscape evolution: Effects of vegetation on landscape processes, drainage density, and topography. *Journal of Geophysical Research: Earth Surface* **110**(F2).

4. Collins D.B.G., Bras R., Tucker G. 2004 Modeling the effects of vegetation-erosion coupling on landscape evolution. *Journal of Geophysical Research: Earth Surface* **109**(F3).
5. Temmerman S., Bouma T., Van de Koppel J., Van der Wal D., De Vries M., Herman P. 2007 Vegetation causes channel erosion in a tidal landscape. *Geology* **35**(7), 631-634.
6. Nardin W., Edmonds D.A. 2014 Optimum vegetation height and density for inorganic sedimentation in deltaic marshes. *Nature Geoscience* **7**(10), 722-726.
7. Kearney W.S., Fagherazzi S. 2016 Salt marsh vegetation promotes efficient tidal channel networks. *Nature Communications* **7**.
8. Baas A., Nield J. 2007 Modelling vegetated dune landscapes. *Geophysical Research Letters* **34**(6).
9. Tal M., Paola C. 2007 Dynamic single-thread channels maintained by the interaction of flow and vegetation. *Geology* **35**(4), 347-350. (doi:10.1130/g23260a.1).
10. Gibling M.R., Davies N.S. 2012 Palaeozoic landscapes shaped by plant evolution. *Nature Geoscience* **5**(2), 99-105.
11. Gurnell A. 2014 Plants as river system engineers. *Earth Surface Processes and Landforms* **39**(1), 4-25.
12. Green J.C. 2005 Modelling flow resistance in vegetated streams: review and development of new theory. *Hydrological processes* **19**(6), 1245-1259.
13. Sand-Jensen K. 1998 Influence of submerged macrophytes on sediment composition and near-bed flow in lowland streams. *Freshwater Biology* **39**(4), 663-679.
14. Cotton J., Wharton G., Bass J., Heppell C., Wotton R. 2006 The effects of seasonal changes to in-stream vegetation cover on patterns of flow and accumulation of sediment. *Geomorphology* **77**(3), 320-334.
15. Wharton G., Cotton J.A., Wotton R.S., Bass J.A., Heppell C.M., Trimmer M., Sanders I.A., Warren L.L. 2006 Macrophytes and suspension-feeding invertebrates modify flows and fine sediments in the Frome and Piddle catchments, Dorset (UK). *Journal of Hydrology* **330**(1), 171-184.
16. Chow V.T. 1959 *Open channel hydraulics*. New York, McGraw-Hill Book Co.; 680 p.
17. Franklin P., Dunbar M., Whitehead P. 2008 Flow controls on lowland river macrophytes: a review. *Science of the Total Environment* **400**(1), 369-378.
18. Puijalon S., Bouma T.J., Douady C.J., van Groenendael J., Anten N.P., Martel E., Bornette G. 2011 Plant resistance to mechanical stress: evidence of an avoidance-tolerance trade-off. *New Phytologist* **191**(4), 1141-1149.
19. Naden P., Rameshwaran P., Mountford O., Robertson C. 2006 The influence of macrophyte growth, typical of eutrophic conditions, on river flow velocities and turbulence production. *Hydrological Processes* **20**(18), 3915-3938.
20. Schoelynck J., De Groote T., Bal K., Vandenbruwaene W., Meire P., Temmerman S. 2012 Self-organised patchiness and scale-dependent bio-geomorphic feedbacks in aquatic river vegetation. *Ecography* **35**(8), 760-768.
21. Cornacchia L., Folkard A., Davies G., Grabowski R.C., van de Koppel J., van der Wal D., Wharton G., Puijalon S., Bouma T.J. 2018 Plants face the flow in V formation: A study of plant patch alignment in streams. *Limnology and oceanography*.
22. Cornacchia L., Van Der Wal D., Van de Koppel J., Puijalon S., Wharton G., Bouma T.J. 2019 Flow-divergence feedbacks control propagule retention by in-stream vegetation: the importance of spatial patterns for facilitation. *Aquatic Sciences* **81**(1), 17.
23. Rietkerk M., Van de Koppel J. 2008 Regular pattern formation in real ecosystems. *Trends in Ecology & Evolution* **23**(3), 169-175.
24. Phillips C.B., Jerolmack D.J. 2016 Self-organization of river channels as a critical filter on climate signals. *Science* **352**(6286), 694-697.

25. Holmes E.E., Lewis M.A., Banks J., Veit R. 1994 Partial differential equations in ecology: spatial interactions and population dynamics. *Ecology* **75**(1), 17-29.
26. Baptist M., Babovic V., Rodríguez Uthurburu J., Keijzer M., Uittenbogaard R., Mynett A., Verwey A. 2007 On inducing equations for vegetation resistance. *Journal of Hydraulic Research* **45**(4), 435-450.
27. Verschoren V., Meire D., Schoelynck J., Buis K., Bal K.D., Troch P., Meire P., Temmerman S. 2016 Resistance and reconfiguration of natural flexible submerged vegetation in hydrodynamic river modelling. *Environmental Fluid Mechanics* **16**(1), 245-265.
28. Stein A., Gerstner K., Kreft H. 2014 Environmental heterogeneity as a universal driver of species richness across taxa, biomes and spatial scales. *Ecology letters* **17**(7), 866-880.
29. Carpenter S.R., Lodge D.M. 1986 Effects of submersed macrophytes on ecosystem processes. *Aquatic botany* **26**, 341-370.
30. Hearne J.W., Armitage P.D. 1993 Implications of the annual macrophyte growth cycle on habitat in rivers. *Regulated Rivers: Research & Management* **8**(4), 313-322. (doi:10.1002/rrr.3450080402).
31. Wharton G., Mohajeri S.H., Righetti M. 2017 The pernicious problem of streambed colmation: a multi-disciplinary reflection on the mechanisms, causes, impacts, and management challenges. *Wiley Interdisciplinary Reviews: Water*.
32. Kemp P., Sear D., Collins A., Naden P., Jones I. 2011 The impacts of fine sediment on riverine fish. *Hydrological Processes* **25**(11), 1800-1821.
33. Corenblit D., Davies N.S., Steiger J., Gibling M.R., Bornette G. 2014 Considering river structure and stability in the light of evolution: feedbacks between riparian vegetation and hydrogeomorphology. *Earth Surface Processes and Landforms* **40**(2), 189-207.
34. Gurnell A.M., Bertoldi W., Corenblit D. 2012 Changing river channels: The roles of hydrological processes, plants and pioneer fluvial landforms in humid temperate, mixed load, gravel bed rivers. *Earth-Science Reviews* **111**(1-2), 129-141.
35. Houghton J.T., Ding Y., Griggs D.J., Noguer M., van der Linden P.J., Dai X., Maskell K., Johnson C.A. 2001 *Climate change 2001: the scientific basis*, The Press Syndicate of the University of Cambridge.
36. Foley J.A., DeFries R., Asner G.P., Barford C., Bonan G., Carpenter S.R., Chapin F.S., Coe M.T., Daily G.C., Gibbs H.K. 2005 Global consequences of land use. *Science* **309**(5734), 570-574.
37. Palmer M.A., Reidy Liermann C.A., Nilsson C., Flörke M., Alcamo J., Lake P.S., Bond N. 2008 Climate change and the world's river basins: anticipating management options. *Frontiers in Ecology and the Environment* **6**(2), 81-89.
38. Sukhodolov A.N., Sukhodolova T.A. 2009 Case study: Effect of submerged aquatic plants on turbulence structure in a lowland river. *Journal of Hydraulic Engineering* **136**(7), 434-446.
39. Vandenbruwaene W., Temmerman S., Bouma T., Klaassen P., De Vries M., Callaghan D., Van Steeg P., Dekker F., Van Duren L., Martini E. 2011 Flow interaction with dynamic vegetation patches: Implications for biogeomorphic evolution of a tidal landscape. *Journal of Geophysical Research: Earth Surface* **116**(F1).
40. Weerman E.J., Van de Koppel J., Eppinga M.B., Montserrat F., Liu Q.X., Herman P.M. 2010 Spatial Self-Organization on Intertidal Mudflats through Biophysical Stress Divergence. *The American Naturalist* **176**(1), E15-E32.
41. Larsen L.G., Harvey J.W., Crimaldi J.P. 2007 A delicate balance: ecohydrological feedbacks governing landscape morphology in a lotic peatland. *Ecological monographs* **77**(4), 591-614.

42. Riis T., Biggs B.J.F. 2003 Hydrologic and hydraulic control of macrophyte establishment and performance in streams. *Limnology and Oceanography* **48**(4), 1488-1497.
43. Vreugdenhil C.B. 1989 *Computational hydraulics: an introduction*, Springer Science & Business Media.
44. Straatsma M.W., Baptist M. 2008 Floodplain roughness parameterization using airborne laser scanning and spectral remote sensing. *Remote Sensing of Environment* **112**(3), 1062-1080.
45. Sand-Jensen K. 2003 Drag and reconfiguration of freshwater macrophytes. *Freshwater Biology* **48**(2), 271-283.
46. Gregg W.W., Rose F.L. 1982 The effects of aquatic macrophytes on the stream microenvironment. *Aquatic botany* **14**, 309-324.
47. Vargas-Luna A., Crosato A., Uijttewaalt W.S. 2015 Effects of vegetation on flow and sediment transport: comparative analyses and validation of predicting models. *Earth Surface Processes and Landforms* **40**(2), 157-176.
48. Schoelynck J., Meire D., Bal K., Buis K., Troch P., Bouma T., Meire P., Temmerman S. 2013 Submerged macrophytes avoiding a negative feedback in reaction to hydrodynamic stress. *Limnologica-Ecology and Management of Inland Waters* **43**(5), 371-380.
49. Bal K.D., Bouma T.J., Buis K., Struyf E., Jonas S., Backx H., Meire P. 2011 Trade-off between drag reduction and light interception of macrophytes: comparing five aquatic plants with contrasting morphology. *Functional Ecology* **25**(6), 1197-1205.
50. Sand-Jensen K., Madsen T.V. 1992 Patch dynamics of the stream macrophyte, *Callitriche cophocarpa*. *Freshwater Biology* **27**(2), 277-282.
51. Rinaldi M., Gurnell A., Del Tánago M.G., Bussetti M., Hendriks D. 2016 Classification of river morphology and hydrology to support management and restoration. *Aquatic sciences* **78**(1), 17-33.
52. Dingman S.L. 1984 *Fluvial hydrology*. New York, 383 pp. WH Freeman, New York; 383 pp. p.
53. Gordon N.D., McMahon T.A., Finlayson B.L., Gippel C.J., Nathan R.J. 2004 *Stream hydrology: an introduction for ecologists*, John Wiley and Sons.
54. Vreugdenhil C.B. 2013 *Numerical methods for shallow-water flow*, Springer Science & Business Media.
55. Koppel J.v.d., Rietkerk M., Dankers N., Herman P.M. 2005 Scale-dependent feedback and regular spatial patterns in young mussel beds. *The American Naturalist* **165**(3), E66-E77.

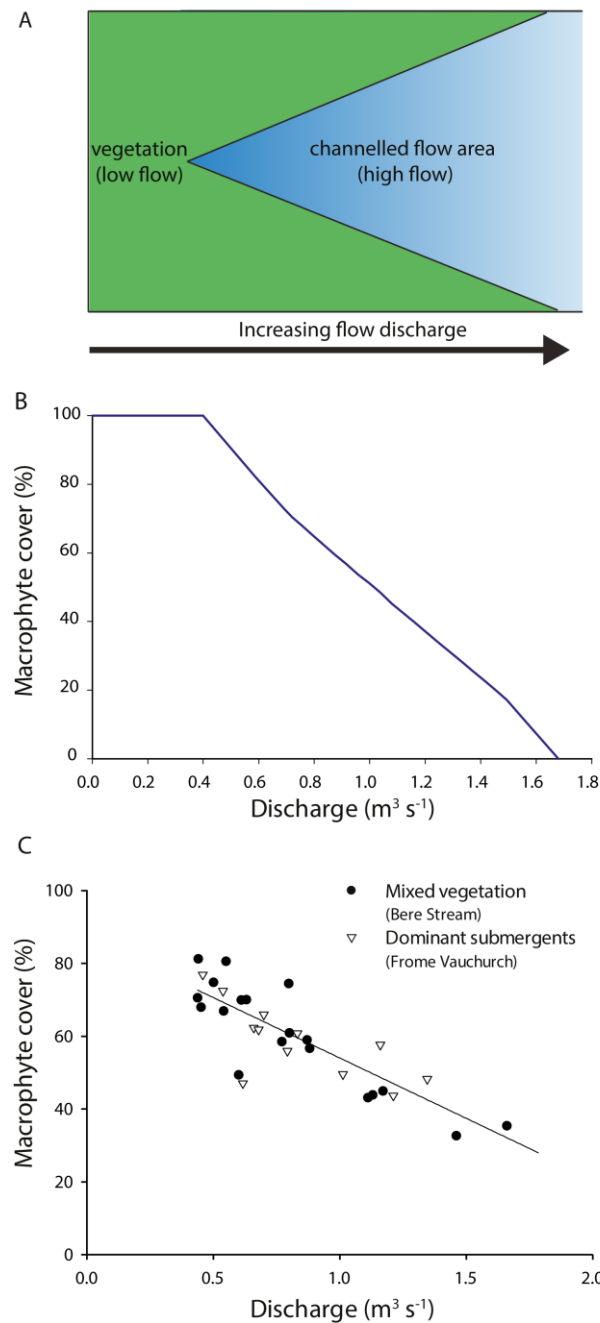


Fig. 1: Relationship between discharge and macrophyte cover in the model and in two chalk streams. (A) Schematic diagram of the “abstract” stream simulated in the model: the proportion of the stream cross-section that is vegetated adjusts in response to changes in water discharge. In the model, at very low discharge, the entire stream cross-section is homogeneously vegetated. As discharge increases, the stream becomes spatially separated into densely vegetated, low-flow zones, and low-density, high-flow zones; vegetation cover decreases until the stream becomes entirely unvegetated. **(B)** Relationship between modelled percentage macrophyte cover (fraction of vegetated cells over the whole simulated domain) and discharge. **(C)** Relationship between macrophyte cover and river discharge as found in the field for both study sites ($N = 31$) ($R^2 = 0.77$, $p < 0.0001$).

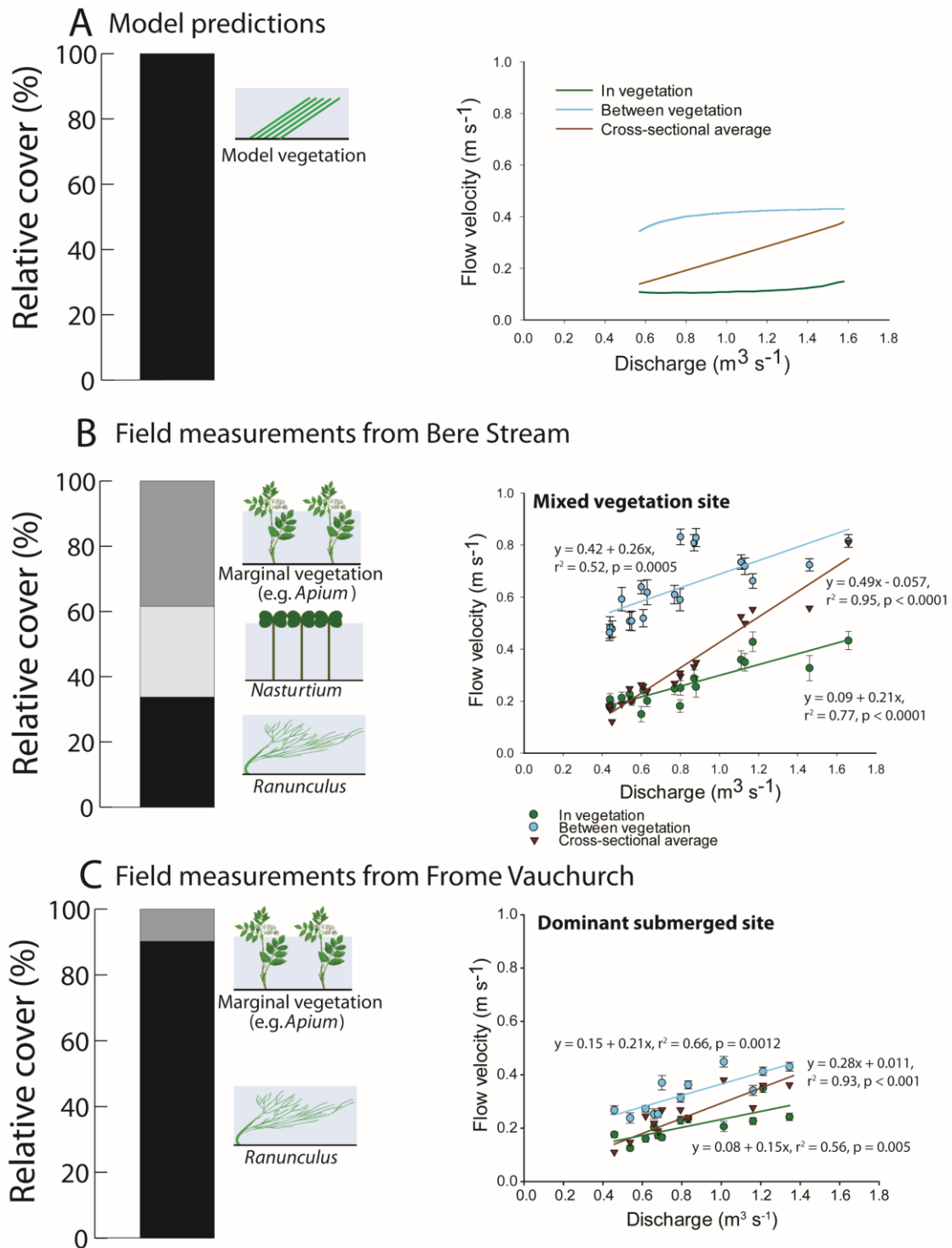
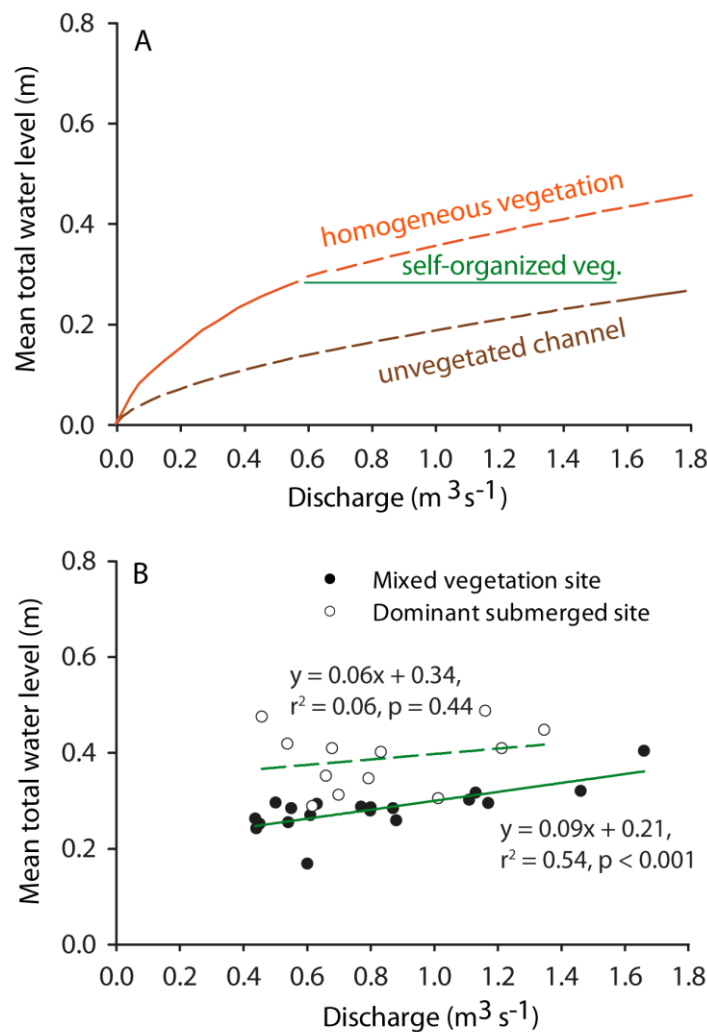


Fig. 2: Relationship between discharge and flow velocity in the model and in two chalk streams. (A) Left: Schematic representation of the flexible submerged aquatic vegetation considered in the model. Right: Model predictions of average flow velocities (m s^{-1}) for increasing values of discharge, calculated within vegetated and unvegetated sections of the channel, and compared with cross-sectional average flow velocities. **(B)** Left: Species composition, expressed as relative macrophyte cover (%) per vegetation type, at the peak of the growing season (July 2008): marginal vegetation (e.g. *Apium*, emergent along the margins), *Nasturtium* (emergent along the margins) and *Ranunculus* (submerged, growing in mid-channel). Right: relationship between flow discharge ($\text{m}^3 \text{s}^{-1}$) and flow velocity (m s^{-1}) in both vegetated and unvegetated river portions in the mixed vegetation site, compared with the cross-sectional average flow velocity in the stream. **(C)** Left: Species composition, expressed as relative macrophyte cover (%)

587 per vegetation type, at the peak of the growing season (July 2008): marginal vegetation (e.g. *Apium*,
588 emergent along the margins) and *Ranunculus* (submerged, growing in mid-channel). *Right*: relationship
589 between flow discharge ($\text{m}^3 \text{s}^{-1}$) and flow velocity (m s^{-1}) in both vegetated and unvegetated river portions
590 in the dominant submerged site, compared with the cross-sectional average flow velocity in the stream.

591



594 **Fig. 3: Relationship between discharge and mean total water level in the model and in two chalk**
 595 **streams. (A)** Model predictions on the relationship between flow discharge ($\text{m}^3 \text{s}^{-1}$) and water level (m)
 596 in the simulated channel with vegetation homogeneously distributed over the channel bed (*orange line*),
 597 with self-organized vegetation (*green line*) and without vegetation (*brown line*). Solid lines indicate the
 598 dominant state over the range of discharge, and dashed lines indicate the relationship outside that range.
 599 **(B)** Field measurements on the relationship between flow discharge ($\text{m}^3 \text{s}^{-1}$) and mean total water level
 600 (m) in the ‘mixed vegetation’ (*solid green line*) and ‘dominant submerged’ (*dashed green line*) study sites.

Table 1. Symbols, interpretations, values, units and sources used in the model simulation.

Symbol	Interpretation	Value	Unit	Source
r	Intrinsic growth rate of plants	1	day ⁻¹	Estimated
k	Carrying capacity of plants	200	g DW m ⁻²	[56]
m_w	Plant mortality coefficient due to water shear stress	3.8	m ⁻¹	Estimated
D	Diffusion rate of plants	0.00085	m ² day ⁻¹	Estimated
n	Manning's roughness coefficient for unvegetated gravel bed	0.025	s/[m ^{1/3}]	[57]
D_c	Drag coefficient	0.04	Dimensionless	[45]
A_w	Wetted plant surface area	$((814.8 * P) - 25.05) * 0.0001$	m ² m ⁻²	[46]
α	Bending angle of plants	$15.5 * \sqrt{u^2 + v^2}^{-0.38}$	degrees	[49]
L	Shoot length	0.5	m	[49]

Note: P is plant biomass [g DW m⁻²]; u is water velocity in the streamwise (x) direction [m s⁻¹]; v is water velocity in the spanwise (y) direction [m s⁻¹].

Table 2. Location, channel dimensions and flow characteristics of the two study sites.

	Bere Stream	Frome Vauchurch
Site location	50° 44' 11.50" N, 2° 12' 21.42" W	50° 46' 29.95" N, 2° 34' 18.32" W
Average discharge (m ³ s ⁻¹)	0.93	1.07
Peak discharge (m ³ s ⁻¹)	2.5	2.95
Average width (m)	7.0	8.9
Average depth (m)	0.30	0.42
Width: depth ratio	23	21